TOXICOLOGICAL SCIENCES **103(2)**, 298–310 (2008)
doi:10.1093/toxsci/kfn055
Advance Access publication March 18, 2008

Liver Genomic Responses to Ciguatoxin: Evidence for Activation of Phase I and Phase II Detoxification Pathways following an Acute Hypothermic Response in Mice

Jeanine S. Morey,* James C. Ryan,* Marie-Yasmine Bottein Dechraoui,* Amir H. Rezvani,† Edward D. Levin,† Christopher J. Gordon,‡ John S. Ramsdell,* and Frances M. Van Dolah*,[1]

*Marine Biotoxins Program, NOAA Center for Coastal Environmental Health and Biomolecular Research, Charleston, South Carolina 29414; †Department of Psychiatry and Behavioral Sciences, Duke University Medical Center, Durham, North Carolina 27710; and ‡Neurotoxicology Division, U. S. EPA, National Health and Environmental Effects Research Laboratory, Research Triangle Park, North Carolina 27711

Received January 8, 2008; accepted March 11, 2008

Ciguatoxins (CTX) are polyether neurotoxins that target voltage-gated sodium channels and are responsible for ciguatera, the most common fish-borne food poisoning in humans. This study characterizes the global transcriptional response of mouse liver to a symptomatic dose (0.26 ng/g) of the highly potent Pacific ciguatoxin-1 (P-CTX-1). At 1 h post-exposure 2.4% of features on a 44K whole genome array were differentially expressed ($p \leq 0.0001$), increasing to 5.2% at 4 h and decreasing to 1.4% by 24 h post-CTX exposure. Data were filtered (|fold change| ≥ 1.5 and $p \leq 0.0001$ in at least one time point) and a trend set of 1550 genes were used for further analysis. Early gene expression was likely influenced prominently by an acute 4°C decline in core body temperature by 1 h, which resolved by 8 h following exposure. An initial downregulation of 32 different solute carriers, many involved in sodium transport, was observed. Differential gene expression in pathways involving eicosanoid biosynthesis and cholesterol homeostasis was also noted. Cytochrome P450s (Cyps) were of particular interest due to their role in xenobiotic metabolism. Twenty-seven genes, mostly members of Cyp2 and Cyp4 families, showed significant changes in expression. Many Cyps underwent an initial downregulation at 1 h but were quickly and strongly upregulated at 4 and 24 h post-exposure. In addition to Cyps, increases in several glutathione *S*-transferases were observed, an indication that both phase I and phase II metabolic reactions are involved in the hepatic response to CTX in mice.

Key Words: **cytochrome P450; ciguatoxin; biotoxin; microarray; liver; gene expression; hypothermia.**

Ciguatoxins (CTXs) are lipid soluble, heat stable cyclic polyethers produced by benthic marine dinoflagellates of the genus *Gambierdiscus*. These potent activators of voltage-gated sodium channels are bioaccumulated through trophic transfer in reef associated fish and are responsible for causing ciguatera fish poisoning (CFP) in humans, affecting 50,000–100,000 people each year (Fleming *et al.*, 2006). CFP is the most common marine poisoning and causes acute gastrointestinal and neurological symptoms, including vomiting, diarrhea, abdominal pain, severe localized itching, tingling of extremities and lips, and thermal dysthesia (Lewis, 2006). Symptoms of CFP can last from several weeks to, in some cases, several years. Chronic symptoms include fatigue, weakness, depression, hypersensitivity to repeated exposure, and recurrence of symptoms may occur upon consumption of nontoxic fish or alcohol (Glaziou and Martin, 1992; Lewis, 2001, 2006). Suites of CTX congeners with varying backbone structures have been found to differ regionally and result in CFP with somewhat different symptoms. In the Pacific Ocean, neurological symptoms dominate. Indian Ocean CFP is similar to the Pacific with the addition of hallucinogenic symptoms, whereas gastrointestinal symptoms predominate in the Caribbean (Lewis, 2006).

Pacific ciguatoxin-1 (P-CTX-1) is the most potent known CTX and is the major congener found in carnivorous fish of the region and, consequently, the predominant source of CFP in the Pacific (Lewis, 2006). It is believed to be a fish metabolite derived from oxidation of the parent CTX4A and CTX4B (formerly called gambiertoxin) produced by *Gambierdiscus* spp. from the Pacific region (Yasumoto and Murata, 1993). This conversion results in 10 times more toxic potency to mammals than the parent compounds, with 0.1 ng CTX/g fish flesh eliciting symptoms in humans (Lehane and Lewis, 2000). The 24 h LD_{50} of P-CTX-1 by ip injection in mice is 0.33 ng/g (Dechraoui *et al.*, 1999).

The metabolism of CTX in mammals has received almost no investigation, primarily because of the lack of purified toxin available to carry out such studies. The persistent and recurrent

[1] To whom correspondence should be addressed at NOAA/NOS/CCEHBR, 219 Fort Johnson Rd., Charleston, SC 29412. Fax: (843) 762-8700. E-mail: Fran.VanDolah@noaa.gov.

nature of ciguatera symptoms raises the possibility that CTX and/or its metabolites may be stored and later mobilized. Therefore, insight into the genomic response to CTX is important to understanding both acute and chronic phases of ciguatera poisoning. In a companion paper (Ryan *et al*., 2007), we characterized the mouse immune response to CTX over an acute time course and identified a predominantly Th2 immune response, indicating an anti-inflammatory environment over the first 24 h following CTX exposure. In a Th2 response, helper T cells direct an immune environment that is thought to be neuroprotective and may be advantageous to preventing neuronal damage during exposure to CTX. In the current study, we use oligonucleotide microarrays and real-time PCR to investigate the pathways in mouse liver responsive to P-CTX-1 over the same time course and, where relevant, relate the concurrent responses observed in liver to the global immune environment.

A key function of the liver is to metabolize xenobiotics. This generally includes the biotransformation of lipophilic substances into more water-soluble metabolites prior to excretion. The reactions to accomplish this are categorized into three phases, hydroxylation (phase I), conjugation (phase II), and transport (phase III). The cytochrome P450s (Cyps) are a superfamily of heme proteins that are the main enzymatic system for the metabolism of lipophilic substrates of varied structures (Nebert and Russell, 2002; Nelson *et al*., 1996). Together with other oxidases, reductases, and dehydrogenases, Cyps are the primary enzyme system responsible for phase I reactions in the hepatic system (Ziegler, 1994). Cyps catalyze the attachment of a hydroxyl group to xenobiotics which can then be used to facilitate phase II reactions, including glucuronidation, sulfation, methylation, attachment of glutathione, N-acetylation, or conjugation with amino acids (Handschin and Meyer, 2003). Finally, in phase III reactions, transporter proteins aid in the excretion of the metabolized xenobiotic.

Although the role of Cyps and other drug-metabolizing enzyme systems in the mammalian response to CTX have not been investigated, studies have been carried out on a structurally related cyclic polyether toxin, brevetoxin, which acts on the same site on voltage-gated sodium channels. Exposure of striped bass to brevetoxin congener PbTx-2 has been shown to increase the activity of CYP1a, a phase I enzyme, and glutathione S-transferase (GST), a phase II enzyme (Washburn *et al*., 1996). *In vitro* studies demonstrate that CYP1a2, CYP2a2, CYP2c11, CYP2d1, and CYP3a1 are all able to catalyze the metabolism of PbTx-2 in rat hepatocytes (Radwan and Ramsdell, 2006). In the only study of transcriptional profiling in mouse liver following PbTx exposure, Walsh *et al*. (2003) found few changes in expression, however a Cyp4a14 was induced. Thus, it has been shown that classical pathways are involved in the metabolism of a ladder-like polyether toxin similar to P-CTX-1. In this study the relative genomic responses of liver to these marine toxins are further evaluated.

MATERIALS AND METHODS

Exposure to P-CTX-1. All studies were conducted at Duke University in accordance with institutional and NIH guidelines for the ethical care and use of laboratory animals. Adult male C57/BL6 mice were maintained on a 12:12 h light:dark cycle and were given food and water *ad libitum*. Radio frequency transmitters were implanted in the mice to measure core temperature and motor activity as previously published (Gordon *et al*., 2001). Briefly, mice were anesthetized with ketamine HCl and a sedative analgesic, medetomidine HCl, and the transmitter (TA10TA-F40; Data Science International Sciences, St Paul, MN) was implanted in the abdominal cavity. Following surgery, mice were administered atipamezol HCl ip to counteract the anesthetic effect of ketamine. The mice were allowed at least 10 days of recovery before testing while animal health was monitored.

On the day of exposure, mice were weighed and randomly assigned to control or experimental groups. Three groups of control mice ($n = 3$) were injected ip with a single dose of physiological saline with 1% Tween 60 (vehicle). Three groups of experimental mice ($n = 3$) were injected ip with 0.26 ng/g P-CTX-1 in vehicle. P-CTX-1, obtained from Dr. Richard Lewis (University of Queensland, Australia), was purified from moray eel liver as described in Lewis *et al*. (1991) with > 90% purity. Core temperature and motor activity were collected into 5 min bins as previously published (Bottein Dechraoui *et al*., 2008). At 1, 4, and 24 h post-injection, three experimental mice and three time-matched controls were anesthetized with 50 mg/ml sodium pentobarbital ip. Livers were immediately dissected, flash frozen in liquid nitrogen, and stored at −80°C until RNA processing. Whole blood samples were collected from the orbital sinus at 30 min and by heart puncture at 1, 4, and 24 h and stored in ethylenediaminetetraacetic acid at 4°C until extraction.

Blood CTX concentrations. Extraction of CTX from blood was carried out using the procedure of Bottein Dechraoui *et al*. (2007). Briefly, blood was extracted with acetonitrile, samples were centrifuged and the supernatant collected and evaporated to dryness. The residue was dissolved in methanol. The concentration of CTX equivalents in blood extracts was determined using the N2A cytotoxicity assay as described in detail by Bottein Dechraoui *et al*. (2007).

RNA processing. The livers of the three control mice for each time point were pooled prior to RNA extraction, whereas RNA was extracted from livers of individual CTX-exposed mice. The livers were crushed using a BioPulverizer (BioSpec Products, Inc., Bartlesville, OK) in liquid nitrogen. The crushed tissue was immediately placed in cooled Tri-Reagent (Molecular Research Center, Inc., Cincinnati, OH) and homogenized using a Tissue-Tearor (United Lab Plastics, St Louis, MO) at 25,000 rpm for 1 min on ice. All homogenates were processed according to the manufacturer's protocol. RNA was resuspended in nuclease-free water and cleaned using an RNeasy midi-column (Qiagen, Valencia, CA) according to manufacturer's protocol. RNA was then quantified using a NanoDrop ND-1000 (Wilmington, DE) and qualified on an Agilent 2100 Bioanalyzer (Foster City, CA).

RNA labeling and array hybridization. Four hundred and fifty nanograms of total RNA from control and experimental animals was separately amplified and labeled with either Cy3- or Cy5-labeled CTP (Perkin Elmer, Waltham, MA) using Agilent's Low Input Linear Amplification kit according to manufacturer's protocol. Following labeling and clean up, amplified RNA and dye incorporation were quantified using a NanoDrop ND-1000. One microgram each of Cy3- and Cy5-labeled targets were combined and hybridized to an Agilent catalog 44K whole genome mouse oligonucleotide array for 17 h at 60°C. After hybridization, arrays were washed consecutively in solutions of 6× saline-sodium phosphate-EDTA buffer (SSPE) with 0.005% N-lauroylsarcosine and 0.06× SSPE with 0.005% N-lauroylsarcosine for 1 min each at room temperature. This was followed by a final 30 s wash in Agilent Stabilization and Drying solution. Three biological replicates, including a dye swap, were performed at each time point.

Microarray analysis. Microarrays were imaged on an Agilent microarray scanner, extracted with Agilent Feature Extraction software version A8.5.1, and

data analyzed with Rosetta Resolver 5.1 gene expression analysis system (Rosetta Informatics, Seattle, WA) using Agilent Design File 012694_D_G2_20051010. Features were subjected to a combination linear and LOWESS normalization algorithm using a rank consistency filter. Resolver generated a weighted average composite array from the replicates ($n = 3$) for each time point based on the error model for the Agilent platform (Weng *et al*., 2006). The composite arrays were used for a trend analysis to determine the expression pattern of genes throughout the time course. Only features with absolute differential expression of 1.5 fold or greater and a composite p value $\leq 10^{-4}$ in at least one time point were included in trend analyses. These data were then clustered using a Euclidean metric by a *K*-means clustering algorithm. The trend set was further analyzed using web tool DAVID (Database for Annotation, Visualization and Integrated Discovery) to identify biological themes in the data set (Dennis *et al*., 2003). DAVID calculates a modified Fisher Exact p value to demonstrate gene enrichment, where p values less than 0.05 are considered to be strongly enriched in the annotation category. A sequence set of all array features with DAVID IDs was used as the background for enrichment analyses. Untrended data from the composite arrays was analyzed in GenMAPP (Gene Map Annotator and Pathway Profiler, Dahlquist *et al*., 2002; Doniger *et al*., 2003; Salomonis *et al*., 2007) to elucidate and visualize differentially expressed pathways in the data set.

Quantitative real-time PCR. Differentially expressed genes of interest were selected for validation of the microarray results by quantitative real-time PCR (qPCR). Triplicate reverse transcription reactions were carried out using 500 ng total RNA with an oligo(dT) primer using Ambion's RETROscript Kit (Austin, TX). Gene specific primers (Supplementary Table 1) were used for qPCR on an ABI 7500 using the ABI Power SYBR Green master mix (Applied Biosystems, Foster City, CA). The optimal annealing temperature for each primer set was determined prior to the analysis of experimental samples. The specificity of each primer set and size of the amplicon were verified by analysis with Agilent's Bioanalyzer 2100 and further confirmed by melting curve analysis. The efficiency of each primer set was determined using a serial dilution series of complimentary DNA (cDNA) from mouse liver. Duplicate 25 µl qPCR reactions were run from each cDNA triplicate. A cycle threshold (C_t) was assigned at the beginning of the logarithmic phase of PCR amplification and the difference in the C_t values of the control and experimental samples were used to determine the relative expression of the gene in each sample. Transmembrane protein 59 was used for normalization as its expression did not change significantly in microarray or qPCR experiments (ANOVA, $p > 0.05$). As data were not normally distributed (Shapiro–Wilk W test), correlation to the microarray data set was determined by Spearman's rho using JMP version 5.1.2 (SAS Institute, Cary, NC).

RESULTS

Mouse Symptomatic Responses

The ip P-CTX-1 dose used in this study is approximately 80% of the LD_{50} in mice. All CTX exposed mice showed hallmark symptoms of CTX exposure that were absent from the time-matched controls, however no mortality was observed. Early responses included diarrhea, piloerection, lacrimation, and hypoactivity. All treated mice showed a rapid depression in core body temperature (Fig. 1), which reached a minimum of 33°C at 1 h and slowly returned to basal temperature (37°C) by 8 h. Blood concentrations of CTX decreased rapidly from 26 pg equiv./ml at 30 min to 7 pg equiv./ml at 4 h, but remained detectable at 24 h at 3 pg equiv./ml (Fig. 2). Blood concentrations in control mice were below the limit of quantification of 0.04 pg equiv./ml (data not shown; Bottein Dechraoui *et al*., 2007). As the N2A cytotoxicity assay measures CTX activity rather than structure, we cannot determine if the decrease observed in the blood is due to clearance or metabolism to less potent forms, or both.

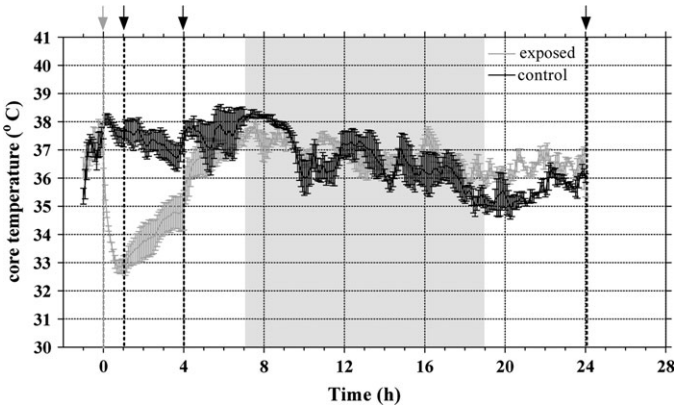

FIG. 1. Core body temperature pre- and post-injection. The core body temperature of all mice was collected in 5 min bins for 1 h pre-injection and continued for 24 h post-injection. Mice were injected with 0.26 ng/g P-CTX-1 (exposed) or vehicle (control) at time 0, as indicated by the gray arrow. Three control and three exposed animals were sacrificed at 1, 4, and 24 h post-injection, as indicated by the black arrows. The dark phase of the 12 h:12 h light:dark cycle is shaded. Values plotted are the mean ± SEM. −1 to 1 h, $n = 9$; 1–4 h, $n = 6$; 4–24 h, $n = 3$.

Microarray Analysis

This study was conducted in a two color format, in which total liver RNA from three individual mice exposed to P-CTX-1 was compared with pooled total liver RNA from time-matched control mice ($n = 3$). The use of a pooled control sample reduces technical variability, but may conceal biological variability in controls and result in higher false predictions for certain genes. The analysis of individual experimental animals provides insight into the biological

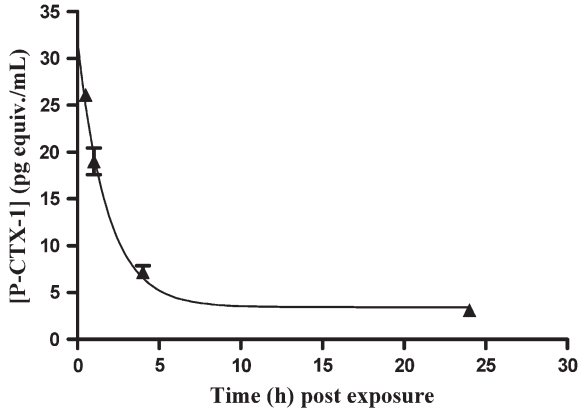

FIG. 2. P-CTX-1 concentration in blood. The P-CTX-1 equivalents in mouse blood following exposure to 0.26 ng/g P-CTX-1 as measured by N2A cytotoxicity assay. Values plotted are the mean ± SEM ($n = 3$).

variability of the response to exposure, which is reflected in the *p* value calculated for a given feature. In addition, coefficient of variation calculations were examined for genes of interest to assess the biological variability. Triplicate arrays from each time point (1, 4, and 24 h) included a dye swap and underwent weighted averaging by Resolver to produce a single composite array at each time point. Using the error model for Agilent arrays, Resolver calculates a *p* value for each feature based on feature intensity, fold change, feature quality and variability between arrays (Weng *et al.*, 2006). A gene was deemed "signature" if the calculated *p* value was 0.0001 or less. At 1 h 979 (2.37%) of genes were called signature, whereas 2152 (5.22%) and 550 (1.35%) were signature at 4 and 24 h, respectively. The ratios of up-:downregulation also varied slightly among time points, with 0.71 at 1 h, 1.11 at 4 h, and 1.04 at 24 h. All raw gene expression data have been deposited in NCBI's Gene Expression Omnibus (GEO, http://www.ncbi.nlm.nih.gov/geo/, GEO Series accession number GSE10768).

Trend analysis. For further analysis of gene expression throughout the time course, a high quality trend set was compiled including only those features that exhibited at least 1.5 fold change and a $p \leq 0.0001$ in at least one time point. This filtering resulted in a trend set of 1550 array probes representing 1366 unique genes (Fig. 3, Supplemental Table 2). The majority of genes (930) qualified for the trend set solely at the 4 h time point. Several genes qualified at two time points (162). Six genes qualified at all three time points: calbindin 3 (s100g), metallothionein 1K, Cyp4a14, apolipoprotein A-IV, farnesyl diphosphate synthetase, and preimplantation protein 4. Because genes that operate within a pathway are often coordinately regulated, the trend set was then clustered by *K*-means using a Euclidean distance metric to discern subsets of genes with similar expression patterns. Membership in a cluster can provide insight into the activation of specific pathways and cross-talk between pathways. In subsequent analyses, the ontology classification of individual clusters indicates several temporally distinct processes initiated in response to CTX.

Cluster 1 contains 400 array probes representing 344 unique genes that, overall, show little change at 1 h, upregulation at 4 h, and varied responses at 24 h (Fig. 3). Analysis with DAVID found this cluster to be enriched with genes classified as cellular physiological process ($p = 2.88E{-}5$, 58.88% of genes) and monooxygenase activity ($p = 2.42E{-}4$, 2.90% of genes) (Table 1). Twelve solute carriers are in this cluster, exhibiting 1.5 to 5.5 fold upregulation at 4 h. Three defensin-related cryptdins were the largest changers, exhibiting 4.1 to 6 fold upregulation by 24 h. Eight Cyps and a Cyp oxidoreductase (Por) are found in cluster 1, with upregulation of 1.6 to 6.5 fold at 4 h and up to 3.9 fold at 24 h. Eight myosin genes present show little change at 1 h, mild upregulation at 4 h (+1.7 to +2.8 fold), and up to 3 fold downregulation by 24 h.

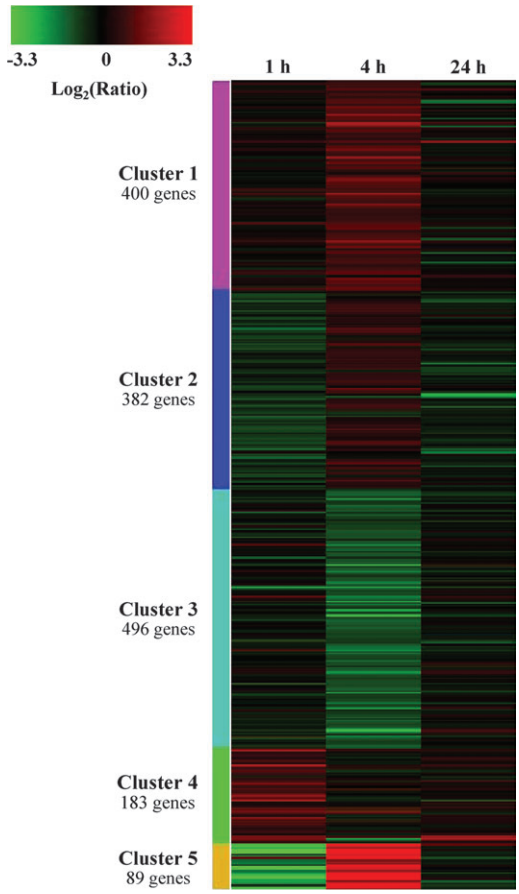

FIG. 3. Cluster analysis of genes used for trending. The 1550 genes comprising the trend set (|fold change| ≥ 1.5 and $p \leq 0.0001$ in at least one time point) were clustered by K-means using a Euclidean metric.

Peroxisome proliferator–activated receptor alpha (PPARα) and two PPARγ cofactors are also found in this cluster and exhibit 1.7 to 2.1 fold upregulation at 4 h.

Cluster 2 contains 382 array probes representing 361 unique genes that exhibit slight downregulation at 1 h, transitioning to upregulation at 4 h, and returning to basal or decreased levels at 24 h (Fig. 3). Gene ontology analysis found that negative regulation of cellular process was the primary biological process ($p = 1.02E{-}4$, 8.12% of genes) and molecular function was found to be enriched for glutathione transferase activity ($p = 4.98E{-}5$, 1.68% of genes) (Table 1). Fifteen solute carriers are present, whose expression profiles differ from the solute carriers in cluster 1 primarily by degree of change, with no to mild downregulation at 1 h (−1.1 to −2.1 fold), transient shift to upregulation (+1.3 to +3.8 fold) at 4 h, and varying patterns of change at 24 h (−4.4 to +1.3 fold). Two Cyps are found in this cluster, with Cyp4b1 showing 3.5 fold downregulation at 1 h. Seven glutathione *S*-transferases exhibit slight downregulation at 1 and 24 h with upregulation at 4 h. Three kallikreins exhibit −1.5 to −1.9 fold change at 1 h.

TABLE 1
GO Annotations from DAVID Analysis of Trend Set

	Biological process	*p* Value	%	Molecular function	*p* Value	%
Cluster 1	Cellular physiological process	2.88E−05	58.88	Monooxygenase activity	2.42E−04	2.90
(345)	Muscle contraction	3.52E−04	2.32	Iron ion binding	3.30E−04	4.35
	Negative regulation of apoptosis	4.74E−04	2.90	Inositol or phosphatidylinositol kinase activity	1.48E−03	1.45
Cluster 2	Negative regulation of cellular process	1.20E−04	8.12	Glutathione transferase activity	4.98E−05	1.68
(357)	Negative regulation of cellular physiological process	3.35E−04	7.00	Tissue kallikrein activity	1.88E−03	1.12
	Negative regulation of biological process	4.92E−04	8.12	Catalytic activity	2.50E−03	31.93
Cluster 3	Sterol metabolism	2.43E−11	3.31	GTPase activity	2.29E−03	2.21
(453)	Sterol biosynthesis	6.61E−11	2.43	Catalytic activity	8.04E−03	30.02
	Steroid biosynthesis	8.19E−11	3.31	Isomerase activity	1.29E−02	1.99
Cluster 4	Digestion	1.29E−03	2.37	Purine-nucleoside phosphorylase activity	1.71E−02	1.18
(169)	Response to other organism	1.77E−03	6.51	Pancreatic elastase activity	1.71E−02	1.18
	Alcohol metabolism	3.10E−03	4.73	Elastase activity	2.55E−02	1.18
Cluster 5	Sodium ion transport	5.63E−05	7.14	Symporter activity	5.56E−05	7.14
(84)	Metal ion transport	6.84E−04	9.52	Porter activity	2.30E−04	8.33
	Monovalent inorganic cation transport	1.21E−03	8.33	Electrochemical potential-driven transporter activity	2.36E−04	8.33

Note. The 22806 features with DAVID IDs from the 44K feature array were used as the background population for enrichment analyses. The number of DAVID IDs in each cluster are indicated in parentheses. *p* values are from a Fisher's Exact test performed in DAVID and indicate enrichment. A $p < 0.05$ is considered strongly enriched. % is the percent of genes in the cluster with the given GO annotation

This cluster also includes two probes for a myosin heavy chain exhibiting 5.1 and 6.5 fold downregulation at 24 h.

Cluster 3 is the largest cluster containing 496 probes to 448 unique genes, most showing little change at 1 and 24 h and downregulation at 4 h (Fig. 3). Analysis with DAVID found this cluster to be enriched with genes from the following annotation categories: sterol metabolism ($p = 2.43E{-}11$, 3.31% of genes) and GTPase (guanosine triphosphatase) activity ($p = m2.29E{-}3$, 2.21% of genes) (Table 1). Kallikrein 12 is the largest changer at 1 h (+4.7 fold) and also displays strong downregulation at 4 h (−3.6 fold). Sterol-C4-methyl oxidase-like is the largest downregulated gene at 4 h (−9.5 fold). This cluster contains several chemokine (C-X-C motif) ligands displaying −1.6 to −2.7 fold downregulation at 4 h. Several alpha and beta tubulin isoforms present in cluster 3 show 1.6 to 2.7 fold downregulation at 4 h. Four Cyp genes present are downregulated either at 4 or 24 h (−1.2 to −4.4 fold).

Cluster 4 contains 183 probes representing 171 genes whose expression generally peaked at 1 h post-CTX exposure, returning to baseline thereafter (Fig. 3). Analysis with DAVID found this cluster to be enriched with genes involved in the biological process of digestion ($p = 1.29E{-}3$, 2.37% of genes) and the molecular function of purine-nucleoside phosphorylase activity ($p = 1.71E{-}2$, 1.18% of genes) (Table 1). Acyl-CoA thioesterase 6 is the largest upregulated gene at 1 h post-CTX exposure (+28.7 fold). The acute phase anti-inflammatory pancreatitis-associated protein is the largest downregulated gene at 4 h (−5.6 fold) and the greatest upregulated gene (+9.4 fold) at 24 h. Seven solute carriers are upregulated 1.6 to 5.4 fold at 1 h in this cluster. Two probes for a single Cyp, Cyp51, displayed mild upregulation at 1 h (+1.5 to +1.7 fold) and 24 h (+1.7 to +2.3 fold). A third probe for Cyp51 fell into cluster 3, but exhibited a similar expression profile.

Cluster 5 is the smallest cluster, containing 89 probes representing 82 genes that generally exhibit strong downregulation at 1 h, strong upregulation at 4 h, and variable change at 24 h (Fig. 3). DAVID found this cluster to be enriched with genes involved in sodium ion transport ($p = 5.63E{-}5$, 7.14% of genes) and symporter activity ($p = 5.56E{-}5$, 7.14% of genes) (Table 1). Transmembrane protein 27 was the largest changer at both the 1 and 4 h time points, exhibiting −74.8 and +97.4 fold change, respectively. Defensin beta 1 was strongly downregulated 5.1 fold at 1 h, but strongly upregulated by 11 fold at 4 h, before returning to control levels at 24 h. The nine solute carriers in this cluster, five of which are known to be involved in sodium ion transport, showed strong downregulation at 1 h (−2.3 to −15.5 fold) and strong upregulation (+2.5 to +26.8 fold) by 4 h post-CTX exposure. The expression profiles of solute carriers in cluster 5 differ from those in preceding clusters primarily by their larger degree of downregulation at 1 h and by upregulation at 4 h. Four Cyps showed downregulation at 1 h (−2.3 to −8.6 fold), strong upregulation at 4 h (+5.1 to +15.1 fold) and, with the exception of Cyp4a14 (+7 fold), return to control levels at 24 h. Lipin 1 was the greatest upregulated gene at 1 h (+2.2 fold), increasing to 14.4 fold at 4 h, but returning to baseline by 24 h.

Cytochrome P450s. In all, 117 features on the 44K feature array correspond to Cyps, representing 73 different isoforms of the protein belonging to 17 families and 36 subfamilies. The trend set contained 27 features corresponding to Cyps, representing 19 different isoforms belonging to 10 families and 13 subfamilies (Table 2). Details of the responses of all Cyps on the array are listed in Supplemental Table 3. Within the trend set, the greatest changes were seen in Cyp2j11, Cyp2j13, and Cyp24a1, which were strongly downregulated at 1 h (−3.2 to −8.6 fold) and strongly upregulated at 4 h (+7.3 to +15 fold), returning to baseline at 24 h. However, the reported magnitude of some of these changes was biased by a single animal (fold change coefficient of variation (CV) > 0.5, Table 2). Cyp2b9, Cyp2b10, and Cyp2b13 were also strongly upregulated at 4 h (+2.6 to +6.5 fold), returning to baseline at 24 h. Cyp4 family members, Cyp4a10, Cyp4a14, and Cyp4a31 were also strongly upregulated at 4 h but remained elevated at 24 h. Cyp39a1 showed a similar pattern, although more modest in response. Fewer Cyps showed significant downregulation. Cyp26a1 was significantly down at 4 h (−4 fold). Three probes for Cyp51 show a tendency toward upregulation at 1 h, down at 4 h, and increased expression again at 24 h. Where discrepancies are apparent between multiple probes for the same gene (Supplemental Fig. 3), it is likely due to probe position on the ORF. Limitations to the transcription efficiency of RNA polymerase result in poorer amplification and noisier signals for the 5′ located probes (e.g., for Cyp2j3 the probes are separated by approximately 1300 bp, Cyp7a1 and Cyp51 2200 bp). When PCR confirmation of these genes was carried out using primers located intermediately on the ORF, the PCR results agreed with the average of the two probes on the array.

GenMAPP Pathway Analysis

Expression data from the composite arrays at each time point were imported into GenMAPP version 2.1 and MAPPFinder 2.0 beta to elucidate pathways responsive to P-CTX-1. Most notably, the cholesterol biosynthesis pathway was strongly downregulated 4 h post-CTX exposure, whereas showing little

TABLE 2
Cyp Genes Included in the Trend Set

Sequence name	Accession no.	Fold change, 1 h	*p* Value, 1 h	Fold change, 4 h	*p* Value, 4 h	Fold change, 24 h	*p* Value, 24 h
Cyp2b9	NM_010000	−1.403	1.94E−07	5.595	< 1.00E−45	1.002	0.9816
Cyp2b9	NM_010000	1.037	0.87689	3.508	2.23E−06	−1.020	0.95021
Cyp2b9[a]	NM_009998	−1.093	0.26423	2.613	3.26E−14	−1.031	0.82869
Cyp2b10	NM_009999	−1.302	0.00247	6.453	2.39E−22	1.144	0.39673
Cyp2b13	NM_007813	−1.202	0.03139	5.422	1.25E−40	1.161	0.34223
Cyp2e1	NM_021282	1.028	0.60286	1.628	<1.00E−45	1.314	3.01E−08
Cyp2j9	NM_028979	1.057	0.77224	1.977	5.97E−18	1.076	0.4035
Cyp2j11	XM_131521	−3.191	0.00001	7.266	0.00154	1.100	0.79608
Cyp2j13	NM_145548	−8.609	1.44E−40	15.080	5.03E−12	1.421	0.68313
Cyp24a1	NM_009996	−6.674	0.00516	11.997	1.40E−07	−1.153	0.85439
Cyp26a1	NM_007811	−1.251	0.19293	−4.436	3.31E−08	−1.005	0.96764
Cyp27a1	NM_024264	1.099	0.5301	1.652	1.68E−22	1.322	0.00015
Cyp3a44	NM_177380	1.563	0.00323	−1.160	0.25658	−1.521	3.57E−06
Cyp39a1	NM_018887	−1.319	0.09214	1.570	0.0008	1.546	0.00003
Cyp4a10	NM_010011	−1.749	0.02489	3.742	< 1.00E−45	2.872	2.57E−12
Cyp4a10	NM_010011	−1.316	0.04669	3.665	6.62E−18	3.854	2.45E−08
Cyp4a10	X71478	−1.200	0.40813	2.701	< 1.00E−45	2.689	7.46E−07
Cyp4a12[b]	NM_177406	1.038	0.81421	1.976	3.64E−15	2.143	0.00001
Cyp4a14	NM_007822	−2.319	2.14E−11	5.128	1.67E−21	6.957	2.40E−09
Cyp4a31[c]	NM_201640	−2.175	0.09152	4.592	1.51E−33	4.208	6.10E−09
Cyp4a31[c]	NM_201640	−1.487	0.02651	2.884	4.25E−42	3.012	2.35E−14
Cyp4b1	NM_007823	−3.500	1.53E−09	−1.198	0.16258	−1.112	0.14607
Cyp51	NM_020010	1.700	9.45E−06	−1.280	0.11997	2.316	1.48E−16
Cyp51	NM_020010	1.534	2.12E−09	−1.365	0.00108	1.659	0.02252
Cyp51	AK028815	1.366	0.11714	−2.093	3.41E−13	1.539	0.08491
Cyp7a1	NM_007824	−1.360	0.00511	−1.695	7.15E−13	1.390	0.23002
Cyp8b1	NM_010012	−1.313	0.01685	2.827	2.94E−19	1.446	0.25788

Note. Shaded values indicate data that met the fold change (≥ |1.5|) and p-value (≤ 0.0001) criteria required for trending, in addition to meeting a fold change coefficient of variation (< 0.5) criteria.

[a]Annotated as Cyp2b10 in Agilent design file 012694_D_G2_20051010.

[b]Annotated as Cyp4a10 in Agilent design file 012694_D_G2_20051010.

[c]Annotated as Cyp4a1 in Agilent design file 012694_D_G2_20051010.

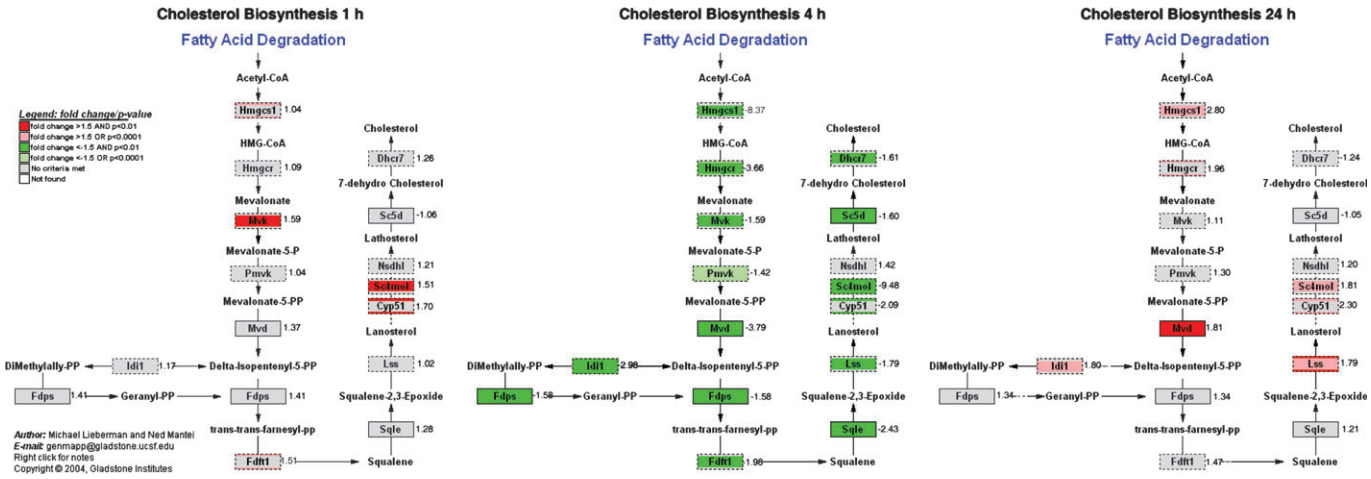

FIG. 4. Changes in the cholesterol biosynthesis pathway in response to CTX. All data from the 44K feature array were input to GenMAPP and MAPPFinder to elucidate any changes in biochemical pathways in response to P-CTX-1 exposure. Cholesterol biosynthesis was found to be strongly downregulated at 4 h post-exposure. This downregulation may be in response to the repression of SREBPs observed at 4 h post-exposure.

change at 1 h or 24 h (Fig. 4). Nearly every gene in the pathway was strongly and/or significantly downregulated, including Cyp51 as noted above. Given this response, it is not surprising that analysis of the quality filtered downregulated genes at the 4 h time point by the functional annotation tool DAVID found enrichment of genes involved in sterol metabolism and biosynthesis ($p = 6.83E{-}10$, 2.64% of genes and $p = 7.76E{-}10$, 1.94% of genes). At 24 h GenMAPP analysis did not indicate significant changes in cholesterol biosynthesis; however, DAVID analysis of filtered upregulated genes at 24 h was found to be significantly enriched for sterol metabolism and biosynthesis ($p = 1.24E{-}7$, 2.00% of genes and $p = 1.31E{-}7$, 1.43% of genes). Upregulation of several myosin, myosin binding, troponin, and actin genes at 4 h resulted in several significant hits in the striated muscle contraction pathway (data not shown). This pathway transitioned to show downregulation by 24 h post-CTX exposure. Likewise, analysis with DAVID of downregulated genes at 24 h indicated that they were enriched for genes involved in muscle contraction ($p = 1.37E{-}3$, 1.38% of genes), the actin cytoskeleton ($p = 5.20E{-}5$, 2.76% of genes), myosin ($p = 5.52E{-}4$, 1.24% of genes), the sarcomere ($p = 1.48E{-}2$, 0.97% of genes), and structural constituents of the cytoskeleton ($p = 4.3E{-}2$, 1.10% of genes).

As the role Cyps play in the metabolism of CTX were of specific interest, the nuclear receptors involved in lipid metabolism and toxicity were interrogated using relaxed filters, to elucidate the possible involvement of multiple Cyps and their corresponding transcription factors (Fig. 5). Overall, limited mild and/or nonsignificant downregulation was observed at 1 h post-exposure. This transitioned to, generally, stronger upregulation at 4 h followed by more modest and/or nonsignificant upregulation by 24 h post-CTX exposure. Nuclear receptors responsive to CTX exposure included PPARα, Nr1i2 (PXR), NR1i3 (CAR), and VDR. VDR was the most extreme in its response with a 4.3 fold decrease at 1 h, then 9 fold increase at 4 h, and 2.8 fold increase at 24 h. Its expression corresponded with the expression patterns of its targets, Cyp24a1 and Cyp3a13. Strong upregulation was also seen in PPARα, which although not included in the pathway map in Figure 5, also regulates Cyps 4a1 and 4a10, two of the most highly upregulated Cyps at 4 h.

qPCR Validation

Eighteen genes were selected for verification by real-time PCR, including transmembrane protein 59, used for normalization (Fig. 6). Tmem59 exhibited minor changes (< 1.2 fold) and good correlation between microarray and qPCR ($\rho = 1.0$, $p < 0.0001$). Overall, the changes in gene expression observed by qPCR strongly supported the microarray results, exhibiting a correlation of 0.93 across the time series ($p < 0.0001$, $n = 54$). The direction of change agreed by both methods for 46 of 54 samples. Where the direction of change was not conserved the magnitude of change was, with one exception (Hmgcs at 1 h), always less than 1.4 fold. Below this threshold of 1.4 fold, increasing disagreement between array and qPCR results has been observed (Morey *et al.*, 2006). At the 1 h time point Cyp2j11 and Cyp24a1 showed much stronger downregulation by qPCR than microarray. The measurements obtained by qPCR were highly repeatable and this discrepancy is likely due to error in the array measurements caused by low spot intensities following strong downregulation of these genes. Even with this disparity in measurements for these 2 genes, the correlation observed between methods at the 1 h time point was 0.86 ($p < 0.0001$, $n = 18$).

DISCUSSION

This study examines the genomic response in liver to a sublethal dose of the highly potent marine neurotoxin,

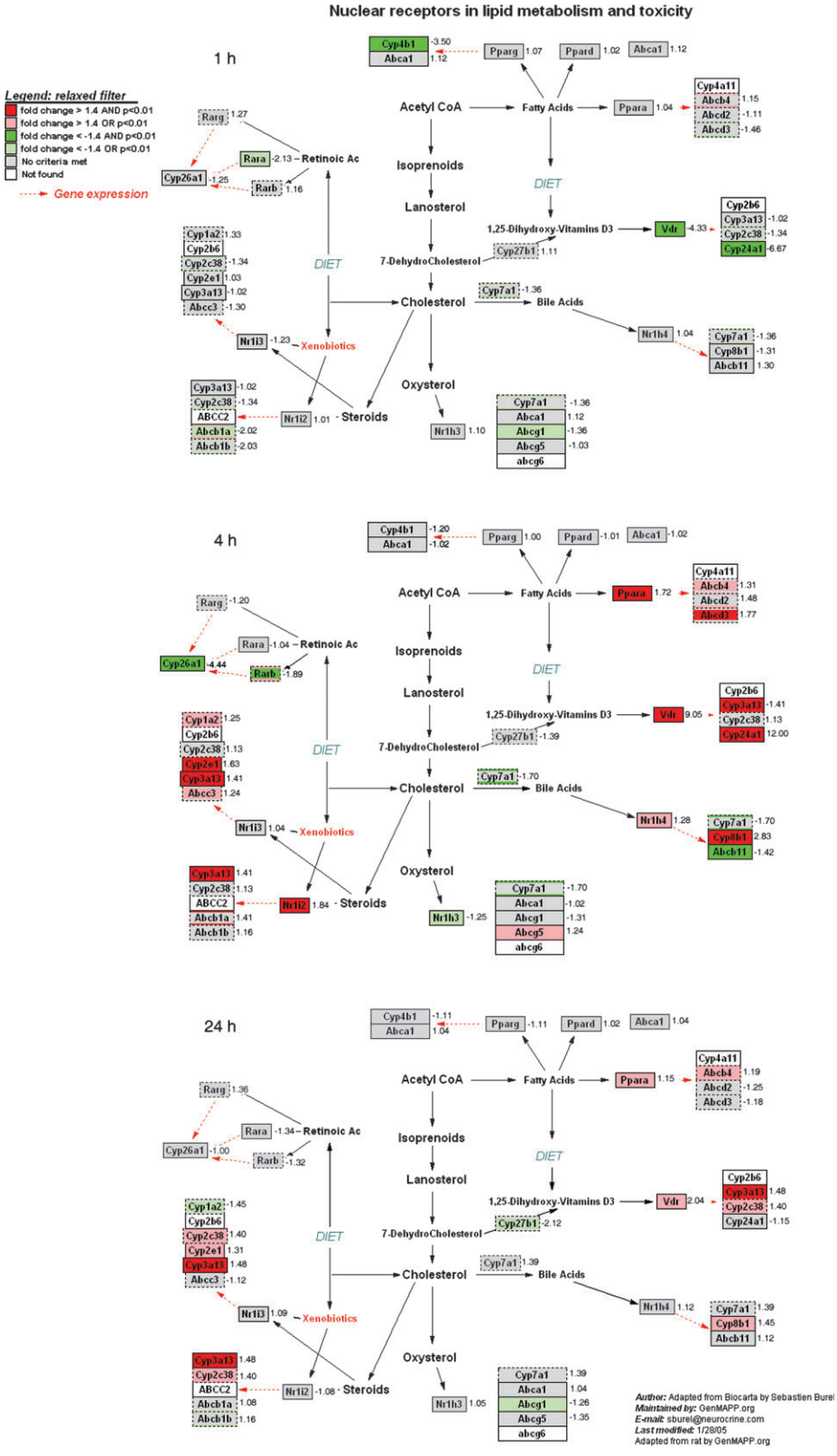

FIG. 5. Changes in Cyps and their associated nuclear receptors in response to CTX. In order to elucidate any changes that may be taking place in phase I detoxification enzymes, a map of nuclear receptors in lipid metabolism and toxicity was generated using a broad filter in GenMAPP and MAPPFinder. Although significant changes were observed in many Cyps, including several not detailed on these maps, only minor and/or nonsignificant changes were observed in the associated nuclear receptors.

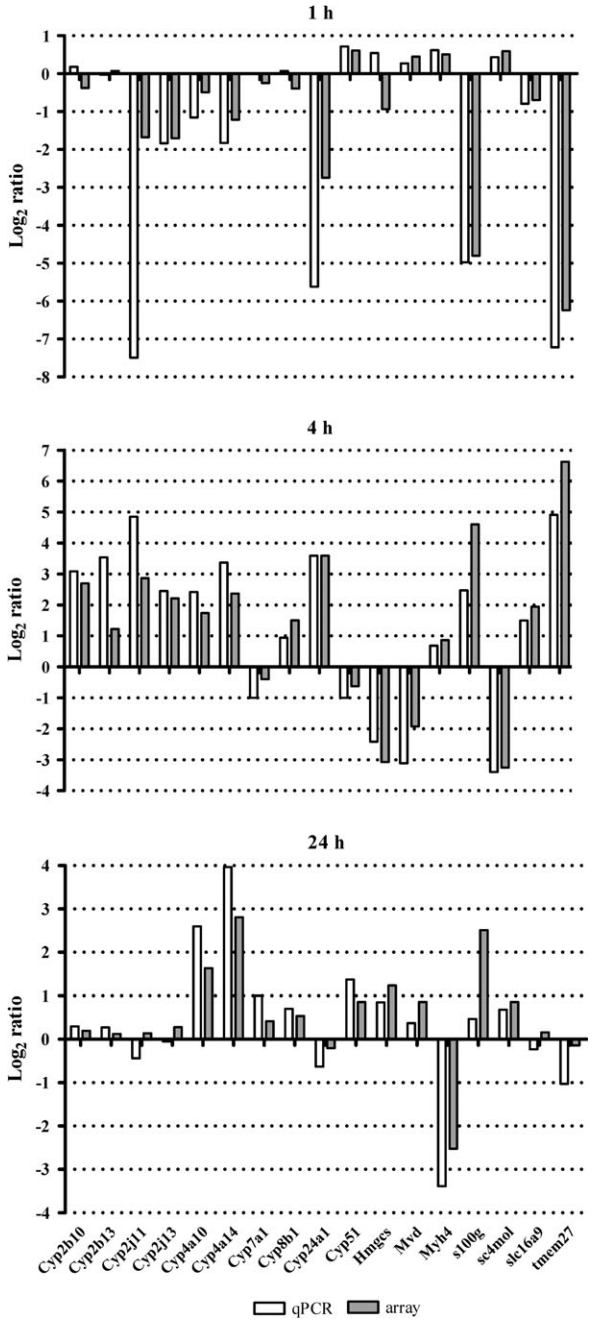

FIG. 6. Validation of microarray results by real-time PCR. Eighteen genes, including one normalizer (not shown), were selected for verification by qPCR. The average value of qPCR assays on triplicate RT reactions and the weighted average from array analyses are plotted. Overall a correlation of 0.93 was observed (Spearman's rho, $p < 0.0001$, $n = 54$). The correlations at the 1, 4, or 24 h time points were 0.86, 0.91, and 0.86, respectively (Spearman's rho, $p < 0.0001$, $n = 18$).

P-CTX-1. The toxic action of CTX is attributed to its potent activation of voltage dependent sodium channels in brain, heart, and muscle, leading to gastrointestinal (vomiting, diarrhea), cardiac, and neurological symptoms that include paresthesia and temperature dysthesia. Although direct targets of CTX are not expected in liver based on its known mode of action, the liver is the major site for detection and detoxification of xenobiotics. In addition, the liver transcriptome is highly responsive to changes in an organism's metabolic state to maintain energy homeostasis. Indeed, we have identified a set of 1550 features from the 44K array that significantly changed in liver over the time course following exposure that are reflective of changing metabolic demands following CTX exposure and activation of detoxification pathways. A major driver of the observed changes in gene expression associated with metabolic homeostasis at early time points following CTX exposure may be an acute suppression in core body temperature. However, no gene expression data is available corresponding to this regulated hypothermic response in mice in response to other intoxicants. Therefore, clarification of which responses are due to hypothermia and which are directly responsive to CTX must await additional studies on genomic responses to other temperature-suppressing xenobiotics.

Core Body Temperature

CTX-treated mice displayed symptoms typical of CTX exposure including diarrhea, piloerection, hypoactivity, and a rapid 4°C decrease in core body temperature, which reached a minimum at 1 h and slowly returned to baseline by 8 h. Structurally related marine polyether toxins, including maitotoxin and brevetoxin, cause similar acute stage hypothermia in mice (Gordon *et al*., 1998, 2001) as do a variety of other xenobiotics including heavy metals, ethanol and organophosphates (Gordon, 1993). This regulated hypothermic response in rodents appears to be a programmed protective mechanism against toxic insult that likely involves CNS thermoregulatory centers that may be direct targets of CTX (Gordon and Ramsdell, 2005). Induced hypothermia has protective effects in liver from ischemic injury by inhibiting the hepatic inflammatory response, through the inhibition of inflammatory cytokines tumor necrosis factor alpha, interleukin 1β (IL1β), and macrophage inflammatory protein 2 (Kato *et al*., 2002). In the current study, IL1β is significantly downregulated (−5.9 fold) in liver by 4 h and remains down at 24 h, whereas other inflammatory cytokines remain unchanged. Similarly, analysis of blood gene expression in the animals from this experiment (Ryan *et al*., 2007) found a predominant Th2, or anti-inflammatory, immune environment throughout this acute phase of CTX exposure with IL 1β downregulated 2.9 fold at 4 h.

Early Responding Genes

The gene expression responses observed at 1 h most likely reflect, in part, metabolic responses to the observed core temperature decrease. A majority of genes responding at 1 h post-exposure exhibited downregulation (up:down ratio 0.71). Solute carriers were highly represented in the gene set responsive at 1 h, with 32 different solute carriers downregulated in response to CTX exposure. These included several organic

anion transporters, cation amino acid transporters, neurotransmitter transporters, and glucose transporters, as well as several transporters, symporters, or cotransporters involved in the movement of sodium. Strong downregulation was observed in Slc34a1, Slc34a3, Slc5a8, and Slc6a18, all involved in the transport of sodium, which transitioned to very strong upregulation by 4 h post-CTX exposure. The organic anion transporters (oatps) play a key role in facilitating hepatic uptake of many chemicals prior to biotransformation in the liver. Downregulation of these transporters may indicate an initial protective response of the liver to prevent excessive damage to the hepatocytes (Cheng *et al*., 2005).

Of note among early upregulated genes were lipin 1 and 2, demonstrating 2 to 3 fold upregulation 1 h post-CTX exposure. Both lipins remained elevated at 4 h, with lipin 1 being among the highest expressors at that time point (+5.3 to +14.4 fold). Lipin 2, by contrast, although remaining up at 4 h (+1.5 to +3.8 fold), appeared to be returning toward baseline. Both lipins were at or below control levels by 24 h. The function of lipins in liver is not fully elucidated, but they are nuclear proteins that play a role in adiposity, glucose homeostasis, and insulin sensitivity (Phan and Reue, 2005). Increased expression of lipins has been shown to be regulated by the PPARγ (Yao-Borengasser *et al*., 2006), which may also impact Cyp expression, however no changes in PPARγ were observed over this time course in response to P-CTX-1. Further, increases in lipin have been shown to activate pathways of mitochondrial fatty acid oxidative metabolism by triggering an induction of PPARα (Finck *et al*., 2006). PPARα was significantly upregulated 1.7 fold 4 h post-CTX exposure, when core temperature was increasing.

Analysis with GenMAPP and MAPPFinder indicated a significant downregulation of cholesterol biosynthesis at 4 h post-CTX exposure. The low-density lipoprotein receptor, not included on this pathway map, but involved in regulating cholesterol levels in the blood, was also significantly downregulated (−2 fold) at 4 h, whereas exhibiting no change at 1 and 24 h. This may be in response to the downregulation of sterol regulatory element-binding proteins (SREBPs, −2.6 fold at 4 h) that are responsible for activating cholesterol biosynthesis (Horton *et al*., 2002). The expression of both SREBPs and most components of the cholesterol biosynthesis pathway had returned to basal levels by 24 h.

Late Responding Genes

By 24 h post-CTX exposure, most genes in the liver had returned to basal expression levels. Exceptions to this trend were several myosin genes, both heavy and light chains, demonstrating −2.2 to −6.5 fold change at 24 h. Likewise, several tropomyosin, troponin, and actin genes were downregulated at 24 h. This is in contrast to the increase of troponin observed in mouse liver 24 h post-brevetoxin exposure (Walsh *et al*., 2003), however an increase in these genes was observed 4 h post-CTX exposure. Sauviat *et al*. (2006) found that P-CTX-1 caused swelling of erythrocytes due to activation of the nitric oxide pathway by inducible nitric oxide synthase. This swelling disrupted the actin cytoskeleton due to elevated intracellular Ca^{2+} and may be a possible cause of downregulation of myosin, tropomyosin, and troponin. In addition, the nitric oxide pathway has been shown to be activated by insulin binding triggered by increased Ca^{2+} levels (Kahn *et al*., 2000). In the current study, the insulin signaling pathway showed a slight induction at 4 h post-CTX exposure in the liver. There are also other indications that oxidative stress may be elevated at that time point including the upregulation of the pro-oxidant Cyp2e1 and several GSTs at 4 h (Kashida *et al*., 2006; Shertzer *et al*., 2004; Yang *et al*., 2002).

Cyp Expression

Cyp enzymes in the liver occupy key positions in the biosynthesis and metabolism of lipids including cholesterol, bile acids, fatty acids, steroids, vitamin D, and eicosanoids. A subset of hepatic Cyps are also responsible for the metabolism of xenobiotics. To date 102 putatively functional Cyp genes have been identified in mouse (Seliskar and Rozman, 2007), many of which have unknown functions. The liver expresses both the greatest number and diversity of Cyps (Choudhary *et al*., 2003). Among these, Cyp families 1–4 are mainly involved in the catabolism of both endogenous lipids and exogenous lipophilic substrates (Gotoh, 1992). The ability of Cyps to metabolize CTX has not previously been investigated and little is known about metabolites in mammals that might shed light on detoxification pathways involved.

The majority (63%) of Cyps included in the current trend set are members of the Cyp2 or Cyp4 families, and the most dramatic changes in Cyp expression were also observed among these families. The Cyp2 and Cyp4 families are known to be highly inducible and differentially expressed following exposure to xenobiotics (Goetz *et al*., 2006; Handschin and Meyer, 2003). However, they also have roles in lipid metabolism that confounds the question of whether they are activated specifically in response to the presence of CTX. In addition, hypothermia is known to suppress the activity of many Cyps (Tortorici *et al*., 2007), however whether the observed decrease in expression (Cyps 2j11, 2j13, 4a1, 4a10, 4a14, and others) is an effect of the acute hypothermic response or the exposure to CTX cannot be determined from the current study. Several members of the Cyp 2 and Cyp 4 families (Cyps 2e1, 2j9, 2j11, 2j13, 4a10, and 4a14) were generally downregulated at 1 h and upregulated at 4 h. Members of the Cyp2 family returned to basal levels by 24 h, whereas member of the Cyp4 family remained upregulated. These genes are involved in the biosynthesis of eicosanoids, and their expression patterns may reflect changes in the metabolic environment concurrent with the hypothermic conditions at 1 h, followed by changes occurring during the return to basal temperature, rather than a direct response to the presence of a xenobiotic substrate.

Cholesterol pathways are commonly disrupted in response to xenobiotic exposure (Handschin and Meyer, 2005). Three Cyps involved in the synthesis of bile acids from cholesterol were upregulated at 4 h or 24 h, Cyp 27a1, Cyp8b1, and Cyp39a1. Conversely, the rate limiting enzyme of this pathway, Cyp7a1, which is feedback regulated by bile acids, was downregulated at 4 h, at the same time that Cyp51 and other members of the cholesterol biosynthesis pathway also were downregulated. Cross-talk between nuclear receptors regulating these endogenous metabolic pathways and those mediating xenobiotic metabolism is widely recognized and not fully understood (Handschin *et al*., 2002; Pascussi *et al*., 2004).

The expression of Cyps is regulated by several ligand-activated transcription factors (Abdel-Razzak *et al*., 1993; Beigneux *et al*., 2002, and others). Of these, the aryl hydrocarbon receptor, constitutively active receptor (CAR), and pregnane X receptor (PXR) are common xenobiotic receptors. The upregulation of Cyps known to be involved in xenobiotic metabolism observed at 4 and 24 h post-exposure may therefore be indicative of their role in phase I metabolism of CTX, with Cyp2b (2b9, 2b10), Cyp2j (2j9, 2j11, 2j13), and Cyp4a (Cyp4a1, Cyp4a10, and Cyp4a14) family members being candidates. Xenobiotics are often classified as activators of specific nuclear receptors, and xenobiotic structure is somewhat predictive of which Cyps may be involved in their metabolism (Morgan *et al*., 1994; Waxman, 1999; Ziegler, 1994). Many structurally diverse compounds activate CAR and PXR and induce transcription of Cyps, most are small in size and highly lipophilic (Handschin and Meyer, 2005). However, in the absence of studies on the direct activation of these nuclear receptors of Cyps by CTX or other polyethers, it is not known if the observed changes are a direct or indirect response to P-CTX-1.

Cyp2 family members are generally considered to be regulated by constitutively expressed CAR and inducible PXR, which form heterodimers. When the current data set was interrogated, PXR (Nr1i3 in Fig. 5) was upregulated at 4 h, whereas CAR (Nr1i2) was constitutively expressed as expected, concurrent with the maximal expression of these Cyp2 family members. Similarly, PPARα was upregulated at 4 h, concurrently with its Cyp4 targets. Several other nuclear receptors demonstrated coordinate expression with their targets, including retinoic acid receptor RAR β, which was downregulated coordinately with Cyp26a1. Strong changes were also observed in the vitamin D receptor (VDR), which is very closely related to the xenobiotic-activated nuclear receptors and can activate several Cyp genes, including the Cyp2b family (Handschin and Meyer, 2005). VDR was downregulated 4.3 fold at 1 h and was strongly upregulated later in the time course (9.1 fold at 4 h and 2.1 fold at 24 h), an expression pattern mirrored by Cyp2b9 and Cyp2b10, as well as Cyp24a, a mitochondrial vitamin D hydroxylase, which was highly upregulated at 4 h.

A compendium of hepatic gene expression in response to a wide array of xenobiotic compounds provides further insight into the complexity of cross-talk between these induction pathways (Slatter *et al*., 2006). Unfortunately, most hepatic gene expression data is carried out following repeat exposures or chronic exposure over multiple days, with gene expression interrogated at 8–24 h following the final dose, such that correlative analysis of the current results is not straightforward. To our knowledge this is the first study to interrogate hepatic gene expression during an acute hypothermic response to intoxication in mice. Comparative studies will be needed to clarify if the upregulation of the candidate Cyps are specific to CTX or if they are a regulated response to the recovery phase of hypothermia.

Comparison with Other Polyether Phycotoxins

Brevetoxin is a polyether toxin of similar structure as CTX and similarly activates voltage dependent sodium channels. Studies in mice have shown that brevetoxin also causes a hypothermic response very similar to that observed following CTX exposure (Gordon and Ramsdell, 2005). *In vitro* studies of rat hepatocytes showed that CYP1a2, CYP2a2, CYP2c11, CYP2d1, and CYP3a1 can metabolize brevetoxin-2 (Radwan and Ramsdell, 2006). However, these genes either showed no change in expression or were not included on the array used in the current study. The absence of change in these Cyps may be attributed to differences in the toxins tested, species-specific differences in Cyp function, or post-transcriptional regulation of their activity. Walsh *et al*. (2003) investigated the effects of brevetoxin congeners PbTx-2 and -6 on gene expression in mouse liver, using similar sub-LD_{50} doses ip. Gene expression was interrogated at 8, 24, and 72 h following exposure. Only 0.3% of features were found to exhibit differential expression in their study. If we apply the higher 1.74 fold cut-off used in Walsh's study to our CTX data, CTX appears to illicit a much stronger response than does brevetoxin, with 2.6% of features found to be differentially expressed following exposure to P-CTX-1. Interestingly, a 2.4 fold increase in Cyp4a14 was observed following 24 h exposure to brevetoxin-6. Cyp4a14 was upregulated 5 and 7 fold at 4 and 24 h in the current study. The differences between hepatic responsiveness to these toxins may reflect the time points queried as previous studies have shown that, in rats, PbTx-2 is mostly cleared to the urine within 24 h and greater than 80% of PbTx-2 is metabolized within 4 h in rat hepatocytes (Radwan and Ramsdell, 2006; Radwan *et al*., 2005). Preliminary studies from our lab indicate that PbTx-3 delivered ip at approximately 75% of the LD_{50} yields moderate changes in liver gene expression 4 h post-exposure. However, many interesting parallels are observed in response to the two different toxins. Many of the strongest downregulated genes 4 h post-PbTx-3 exposure are solute carriers involved in the transport of sodium, whereas lipin 1 and an oxidative stress response gene are strongly upregulated (Morey *et al*., unpublished data). Although in response to PbTx-3 only 10 Cyps meet the fold change and *p* value filters used in this study, the

trends observed are similar to those seen following CTX exposure. Cyp7a1 and Cyp51 are significantly downregulated 4 h post-exposure to either toxin. In contrast, Cyps 2j6, 4a1, 4a10, and 4a14 and Cyp oxidoreductase are all significantly upregulated in response to both brevetoxin and CTX (Morey *et al*., unpublished data). A number of genes involved with cholesterol biosynthesis were downregulated 4 h post-CTX exposure in this study. No changes in these genes were observed 4 h post-brevetoxin exposure (Morey *et al*., unpublished data). It is interesting to note that azaspiracid, a polyether marine phycotoxin, caused significant upregulation of the cholesterol biosynthesis pathway in an *in vitro* study of human lymphocytes (Twiner *et al*., 2008).

CONCLUSIONS

Despite the prevalence of CFP as a worldwide foodborne illness, the toxicological responses to CTX have received little attention due to the limited availability of purified toxin for such studies. This study provides the first insight into liver responses to the lipophilic polyether P-CTX-1 using a toxicogenomic approach. Several solute carriers, many involved in sodium transport, were downregulated 1 h post-exposure. Throughout the time course, differential gene expression in pathways involving eicosanoid biosynthesis and cholesterol homeostasis was observed. Following initial downregulation that corresponds with the acute hypothermic response in mice to intoxication, the strong responses of several Cyps at 4 and 24 h identified candidates for a role in phase I detoxification. Several phase II enzymes were also induced 4 h following exposure. This study may provide the basis for a further understanding of the detoxification of a potent marine toxin in mammalian systems.

SUPPLEMENTARY DATA

Supplementary data are available online at http://toxsci.oxfordjournals.org/.

ACKNOWLEDGMENTS

We would like to thank J. Tiedeken and M. Peterson for help with the experimental procedure.

REFERENCES

Abdel-Razzak, Z., Loyer, P., Fautrel, A., Gautier, J. C., Corcos, L., Turlin, B., Beaune, P., and Guillouzo, A. (1993). Cytokines down-regulate expression of major cytochrome P-450 enzymes in adult human hepatocytes in primary culture. *Mol. Pharmacol.* **44,** 707–715.

Beigneux, A. P., Moser, A. H., Shigenaga, J. K., Grunfeld, C., and Feingold, K. R. (2002). Reduction in cytochrome P-450 enzyme expression is associated with repression of CAR (constitutive androstane receptor) and PXR (pregnane X receptor) in mouse liver during the acute phase response. *Biochem. Biophys. Res. Commun.* **293,** 145–149.

Bottein Dechraoui, M.-Y., Rezvani, A. H., Gordon, C. J., Levin, E. D., and Ramsdell, J. S. (2008). Repeat exposure to ciguatoxin leads to enhanced and sustained thermoregulatory, pain threshold and motor activity responses in mice: Relationship to blood ciguatoxin concentrations. *Toxicology* **246,** 55–62.

Bottein Dechraoui, M.-Y., Wang, Z., and Ramsdell, J. S. (2007). Optimization of ciguatoxin extraction method from blood for Pacific ciguatoxin (P-CTX-1). *Toxicon* **49,** 100–105.

Cheng, X., Maher, J., Dieter, M. Z., and Klaassen, C. D. (2005). Regulation of mouse organic anion-transporting polypeptides (oatps) in liver by prototypical microsomal enzyme inducers that activate distinct transcription factor pathways. *Drug Metab. Dispos.* **33,** 1276–1282.

Choudhary, D., Jansson, I., Schenkman, J. B., Sarfarazi, M., and Stoilov, I. (2003). Comparative expression profiling of 40 mouse cytochrome P450 genes in embryonic and adult tissues. *Arch. Biochem. Biophys.* **414,** 91–100.

Dahlquist, K., Salmonis, N., Vranizan, K., Lawlor, S., and Conklin, B. (2002). GenMAPP, a new tool for viewing and analyzing microarray data on biological pathways. *Nat. Genet.* **31,** 19–20.

Dechraoui, M.-Y., Naar, J., Pauillac, S., and Legrand, A.-M. (1999). Ciguatoxins and brevetoxins, neurotoxic polyether compounds active on sodium channels. *Toxicon* **37,** 125–143.

Dennis, G., Sherman, B., Hosack, D., Yang, J., Gao, W., Lane, H. C., and Lempicki, R. (2003). DAVID: Database for annotation, visualization, and integrated discovery. *Genome Biol.* **4,** P3.

Doniger, S., Salomonis, N., Dahlquist, K., Vranizan, K., Lawlor, S., and Conklin, B. (2003). MAPPFinder: Using gene ontology and GenMAPP to create a global gene-expression profile from microarray data. *Genome Biol.* **4,** R7.

Finck, B. N., Gropler, M. C., Chen, Z., Leone, T. C., Croce, M. A., Harris, T. E., Lawrence, J. J. C., and Kelly, D. P. (2006). Lipin 1 is an inducible amplifier of the hepatic PGC-1α/PPARα regulatory pathway. *Cell Metab.* **4,** 199–210.

Fleming, L. E., Broad, K., Clement, A., Dewailly, E., Elmir, S., Knap, A., Pomponi, S. A., Smith, S., Solo Gabriele, H., *et al.* (2006). Oceans and human health: Emerging public health risks in the marine environment. *Mar. Pollut. Bull.* **53,** 545–560.

Glaziou, P., and Martin, P. (1992). Study of factors that influence the clinical response to ciguatera fish poisoning. *Bull. Soc. Pathol. Exot.* **85,** 419–420.

Goetz, A. K., Bao, W., Ren, H., Schmid, J. E., Tully, D. B., Wood, C., Rockett, J. C., Narotsky, M. G., Sun, G., Lambert, G. R., Thai, S.-F., *et al.* (2006). Gene expression profiling in the liver of CD-1 mice to characterize the hepatotoxicity of triazole fungicides. *Toxicol. Appl. Pharmacol.* **215,** 274–284.

Gordon, C. J. (1993). In *Temperature Regulation in Laboratory Rodents*. Cambridge University Press, New York.

Gordon, C. J., Kimm-Brinson, K. L., Padnos, B., and Ramsdell, J. S. (2001). Acute and delayed thermoregulatory response of mice exposed to brevetoxin. *Toxicon* **39,** 1367–1374.

Gordon, C. J., and Ramsdell, J. S. (2005). Effects of marine algal toxins on thermoregulation in mice. *Neurotoxicol. Teratol.* **27,** 727–731.

Gordon, C. J., Yang, Y., and Ramsdell, J. S. (1998). Behavioral thermoregulatory response to maitotoxin in mice. *Toxicon* **36,** 1341–1347.

Gotoh, O. (1992). Substrate recognition sites in cytochrome P450 family 2 (CYP2) proteins inferred from comparative analyses of amino acid and coding nucleotide sequences. *J. Biol. Chem.* **267,** 83–90.

Handschin, C., and Meyer, U. A. (2003). Induction of drug metabolism: The role of nuclear receptors. *Pharmacol. Rev.* **55,** 649–673.

Handschin, C., and Meyer, U. A. (2005). Regulatory network of lipid-sensing nuclear receptors: Roles for CAR, PXR, LXR, and FXR. *Arch. Biochem. Biophys.* **433,** 387–396.

Handschin, C., Podvinec, M., Amherd, R., Looser, R., Ourlin, J.-C., and Meyer, U. A. (2002). Cholesterol and bile acids regulate xenosensor signaling in drug-mediated induction of cytochromes P450. *J. Biol. Chem.* **277,** 29561–29567.

Horton, J. D., Goldstein, J. L., and Brown, M. S. (2002). SREBPs: Activators of the complete program of cholesterol and fatty acid synthesis in the liver. *J. Clin. Invest.* **109,** 1125–1130.

Kahn, N. N., Acharya, K., Bhattacharya, S., Acharya, R., Mazumder, S., Bauman, W. A., and Sinha, A. K. (2000). Nitric oxide: The "second messenger" of insulin. *IUBMB Life* **49,** 441–450.

Kashida, Y., Takahashi, A., Moto, M., Okamuram, M., Muguruma, M., Jin, M., Arai, K., and Mitsumori, K. (2006). Gene expression analysis in mice liver on hepatocarcinogenesis by flumequine. *Arch. Toxicol.* **80,** 533–539.

Kato, A., Singh, S., McLeish, K. R., Edwards, M. J., and Lentsch, A. B. (2002). Mechanisms of hypothermic protection against ischemic liver injury in mice. *Am. J. Physiol. Gastrointest. Liver Physiol.* **282,** G608–g616.

Lehane, L., and Lewis, R. J. (2000). Ciguatera: Recent advances but the risk remains. *Int. J. Food Microbiol.* **61,** 91–125.

Lewis, R. J. (2001). The changing face of ciguatera. *Toxicon* **39,** 97.

Lewis, R. J. (2006). Ciguatera: Australian perspectives on a global problem. *Toxicon* **48,** 799–809.

Lewis, R. J., Sellin, M., Poli, M. A., Norton, R. S., MacLeod, J. K., and Sheil, M. M. (1991). Purification and characterization of ciguatoxins from moray eel (Lycodontis javanicus, Muraenidae). *Toxicon* **29,** 1115–1127.

Morey, J. S., Ryan, J. C., and Van Dolah, F. M. (2006). Microarray validation: Factors influencing correlation between oligonucleotide microarrays and real-time PCR. *Biol. Proc. Online* **8,** 175–193.

Morgan, E. T., Thomas, K. B., Swanson, R., Vales, T., Hwang, J., and Wright, K. (1994). Selective suppression of cytochrome P-450 gene expression by interleukins 1 and 6 in rat liver. *Biochim. Biophys. Acta Gene Struct. Expr.* **1219,** 475–483.

Nebert, D. W., and Russell, D. W. (2002). Clinical importance of the cytochromes P450. *Lancet* **360,** 1155–1162.

Nelson, D. R., Koymans, L., Kamataki, T., Stegeman, J. J., Feyereisen, R., Waxman, D. J., Waterman, M. R., Gotoh, O., Coon, M. J., Estabrook, R. W., *et al.* (1996). P450 superfamily: Update on new sequences, gene mapping, accession numbers and nomenclature. *Pharmacogenetics* **6,** 1–42.

Pascussi, J. M., Gerbal-Chaloin, S., Drocourt, L., AssÃcnat, E., Larrey, D., Pichard-Garcia, L., Vilarem, M. J., and Maurel, P. (2004). Cross-talk between xenobiotic detoxication and other signalling pathways: Clinical and toxicological consequences. *Xenobiotica* **34,** 633–664.

Phan, J., and Reue, K. (2005). Lipin, a lipodystrophy and obesity gene. *Cell Metab.* **1,** 73–83.

Radwan, F. F. Y., and Ramsdell, J. S. (2006). Characterization of *in vitro* oxidative and conjugative metabolic pathways for brevetoxin (PbTx-2). *Toxicol. Sci.* **89,** 57–65.

Radwan, F. F. Y., Wang, Z., and Ramsdell, J. S. (2005). Identification of a rapid detoxification mechanism for brevetoxin in rats. *Toxicol. Sci.* **85,** 839–846.

Ryan, J. C., Bottein Dechraoui, M.-Y., Morey, J. S., Rezvani, A., Levin, E. D., Gordon, C. J., Ramsdell, J. S., and Van Dolah, F. M. (2007). Transcriptional profiling of whole blood and serum protein analysis of mice exposed to the neurotoxin Pacific ciguatoxin-1. *Neurotoxiciology* **28,** 1099–1109.

Salomonis, N., Hanspers, K., Zambon, A. C., Vranizan, K., Lawlor, S. C., and Dahlquist, K. D. (2007). GenMAPP 2: New features and resources for pathway analysis. *BMC Bioinformatics* **8,** 217–228.

Sauviat, M.-P., Boydron-Le Garrec, R., Masson, J.-B., Lewis, R. L., Vernoux, J.-P., Molgo, J., Laurent, D., and Benoit, E. (2006). Mechanisms involved in the swelling of erythrocytes caused by Pacific and Caribbean ciguatoxins. *Blood Cells Mol. Dis.* **36,** 1–9.

Seliskar, M., and Rozman, D. (2007). Mammalian cytochromes P450—Importance of tissue specificity. *Biochim. Biophys. Acta* **1770,** 458–466.

Shertzer, H. G., Clay, C. D., Genter, M. B., Schneider, S. N., Nebert, D. W., and Dalton, T. P. (2004). CYP1A2 protects against reactive oxygen production in mouse liver microsomes. *Free Radic. Biol. Med.* **36,** 605–617.

Slatter, J. G., Cheng, O., Cornwell, P. D., De Souza, A., Rockett, J., Rushmore, T., Hartley, D., Evers, R., He, Y., Dai, X., *et al.* (2006). Microarray-based compendium of hepatic gene expression profiles for prototypical ADME gene-inducing compounds in rats and mice *in vivo*. *Xenobiotica* **36,** 902–937.

Tortorici, M. A., Kochanek, P. M., and Poloyac, S. M. (2007). Effects of hypothermia on drug disposition, metabolism, and response: A focus of hypothermia-mediated alterations on the cytochrome P450 enzyme system. *Crit. Care Med.* **35,** 2196–2204.

Twiner, M. J., Ryan, J. C., Morey, J. S., Smith, K. J., Hamman, S. M., Van Dolah, F. M., Hess, P., McMahon, T., Satake, M., Yasumoto, T., *et al.* (2008). Transcriptional profiling and inhibition of cholesterol biosynthesis in human lymphocyte T cells by the marine toxin azaspiracid. *Genomics* **91,** 289–300.

Walsh, P. J., Bookman, R. J., Zaias, J., Mayer, G. D., Abraham, W., Bourdelais, A. J., and Baden, D. G. (2003). Toxicogenomic effects of marine brevetoxins in liver and brain of mouse. *Comp. Biochem. Physiol. B Biochem. Mol. Biol.* **136,** 173–182.

Washburn, B. S., Vines, C. A., Baden, D. G., Hinton, D. E., and Walsh, P. J. (1996). Differential effects of brevetoxin and β-naphthoflavone on xenobiotic metabolizing enzymes in striped bass (*Morone saxatilis*). *Aquat. Toxicol.* **35,** 1–10.

Waxman, D. J. (1999). P450 gene induction by structurally diverse xenochemicals: Central role of nuclear receptors CAR, PXR, and PPAR. *Arch. Biochem. Biophys.* **369,** 11–23.

Weng, L., Dai, H., Zhan, Y., He, Y., Stepaniants, S. B., and Bassett, D. E. (2006). Rosetta error model for gene expression analysis. *Bioinformatics* **22,** 1111–1121.

Yang, Y., Sharma, R., Zimniak, P., and Awasthi, Y. C. (2002). Role of α class glutathione s-transferases as antioxidant enzymes in rodent tissues. *Toxicol. Appl. Pharmacol.* **182,** 105–115.

Yao-Borengasser, A., Rasouli, N., Varma, V., Miles, L. M., Phanavanh, B., Starks, T. N., Phan, J., Spencer, H. J., III., McGehee, R. E., Jr., Reue, K., *et al.* (2006). Lipin expression is attenuated in adipose tissue of insulin-resistant human subjects and increases with peroxisome proliferator-activated receptor γ activation. *Diabetes* **55,** 2811–2818.

Yasumoto, T., and Murata, M. (1993). Marine toxins. *Chem. Rev.* **93,** 1897–1909.

Ziegler, D. (1994). Detoxification: Oxidation and reduction. In *The Liver: Biology and Pathobiology* (I. Arias, J. Boyer, N. Fausto, W. Jakoby, D. Schachter, and D. Shafritz, Eds.), pp. 415–427. Raven Press, New York, NY.